JOURNAL OF PROPULSION AND POWER
Vol. 13, No. 2, March–April 1997

# Monte Carlo Probability Density Function Method for Gas Turbine Combustor Flowfield Predictions

Anil K. Tolpadi* and Sanjay M. Correa†
*General Electric Corporate R&D Center, Schenectady, New York 12301*
and
David L. Burrus‡ and Hukam C. Mongia§
*General Electric Aircraft Engines, Cincinnati, Ohio 45215*

**A coupled Lagrangian Monte Carlo (MC) probability density function (PDF), Eulerian computational fluid dynamics (CFD) technique is presented for calculating steady three-dimensional turbulent reacting flow in a gas turbine combustor. PDF transport methods model turbulence–combustion interactions more accurately than conventional turbulence models with an assumed-shape PDF. The PDF was over composition only. The PDF transport equation was solved using a Lagrangian particle-tracking MC method. This MC module has been coupled with CONCERT, which is a fully elliptic three-dimensional body-fitted CFD code based on pressure correction techniques. CONCERT calculates the mean velocity and mixing frequency field that are required by the composition PDF in the MC module, whereas the MC module computes the PDF from which the mean density field is extracted and supplied to CONCERT. This modeling approach was initially validated against Raman data taken in a recirculating bluff body stabilized flame. The computed mixture fraction and its variance (as obtained from the calculated PDF) compared very well against the corresponding measurements made along several radial lines at different axial downstream positions and along the axis. A typical single annular aircraft engine combustor was also analyzed. In this preliminary study, the flowfield, fuel, and temperature distribution were obtained based on the assumption of fast chemistry. The solutions obtained using the present approach were compared with those obtained using a presumed-shape PDF method. The comparison of the calculated exhaust gas temperatures using these two approaches with measurements made by a thermocouple rake appeared to indicate better agreement with the PDF transport technique.**

## Nomenclature

| | | |
|---|---|---|
| $D$ | = | diffusivity used in the random walk, $2\mu_T/\bar{\rho}$ |
| $d$ | = | jet exit diameter, bluff-body flame |
| $k$ | = | turbulent kinetic energy |
| $N_p$ | = | total number of particles in the computational domain |
| $nstep$ | = | particle tracking step-size parameter |
| $Sc$ | = | turbulent Schmidt number |
| $T3$ | = | average combustor inlet temperature |
| $T4$ | = | average combustor exit temperature |
| $t$ | = | time coordinate |
| $x$ | = | axial distance downstream from jet, bluff-body flame |
| $\Delta t$ | = | time step |
| $\varepsilon$ | = | dissipation rate of turbulent kinetic energy |
| $\mu_T$ | = | turbulent viscosity, momentum equations |
| $\bar{\rho}$ | = | mean density calculated for each computational cell |
| $\omega$ | = | mixing frequency, $\varepsilon/k$ |

## Introduction

IN a gas turbine combustor, there exists a wide range of complex, interacting physical and chemical phenomena. Some of these phenomena include 1) finite rate chemistry of combustion, $NO_x$, and CO emissions; 2) turbulent transport; 3) two-phase flow; 4) radiation; and 5) particulate behavior. Depending on the specific issues being addressed, models of varying degrees of sophistication have been employed. The level of sophistication in design models has continually increased over the years, with improvements in numerical methods, computer capabilities, and physical understanding.

The calculation of emissions in practical combustors requires the treatment of finite rate kinetics. It is also necessary to calculate the three-dimensional flowfield in the device. To accurately predict emissions, it is important to account for the effect of turbulent fluctuations. Modeling of combustion with an eddy breakup model is inadequate because it contains limited information about kinetics and ignores turbulent fluctuations. The effect of fluctuations can be modeled using the probability density function (PDF) approach. Current generation computational fluid dynamic (CFD) models for practical combustors typically employ an assumed-shape PDF parameterized by the mean and variance of the mixture fraction.[1–3] Transport equations are solved for each of the mean and variance. The chemistry is assumed to be infinitely fast, although slow reactions can be considered if they are decoupled from the heat release reactions. The density and temperature field are then related to a single conserved scalar. A variety of shapes can be prescribed for the PDF. In Refs. 1–3, a beta PDF was employed. While such an approach makes reasonable predictions[4] of the combustor exit temperature profile and the $NO_x$ emission index, it cannot predict CO, unburnt hydrocarbons (UHC), and other important phenomena such as blowout. It is possible to model finite rate kinetics with multidimensional assumed-shape PDFs, but it is not very practical since the PDF prescription can become very complex with an increase in the number of parameters.

A more promising approach for the solution of turbulent flows with finite rate chemistry is the PDF transport method.[5]

Received May 7, 1995; presented as Paper 95-2443 at the AIAA/ASME/SAE/ASEE 31st Joint Propulsion Conference and Exhibit, San Diego, CA, July 10–12, 1995; revision received May 19, 1996; accepted for publication July 5, 1996. 

*Staff Engineer, P.O. Box 8.
†Manager, Combustion Program, P.O. Box 8. Member AIAA.
‡Staff Engineer, Mail Drop E404. Member AIAA.
§Manager, Combustion Design Engineering, Mail Drop E404. Member AIAA.

The PDF transport method solves the transport equation for a joint PDF of at least the composition variables. The composition PDF eliminates the need to model the mean reaction rates. The mean value of density, temperature, and composition can be obtained from the PDF. Models have to be developed for convection and molecular mixing. The velocity terms can be retained to yield a joint velocity–composition PDF that eliminates the need for gradient transport models, although modeling of the viscous terms and the pressure gradient are required. The mean pressure field can be obtained by solving a Poisson equation for elliptic flows[6] or through the solution obtained by a conventional flow solver.[7] The joint velocity–composition PDF approach was used in calculating a recirculating two-dimensional axisymmetric stabilized flame.[7,8] PDF transport models have also been successfully used in the calculation of a number of simple jet-like turbulent flames.[9–13] Leonard and Dai[14] have performed two-dimensional reacting flow calculations (and compared with data) using a PDF transport model coupled with a general-purpose CFD code. Reduced chemistry schemes of Chen and Kollmann[13] were used and a demonstrative calculation in a three-dimensional generic combustor was also shown.

This paper describes the development of a Monte Carlo (MC) composition PDF module that has been coupled with a fully elliptic three-dimensional body-fitted CFD code based on pressure correction techniques (CONCERT-3D). CONCERT-3D has been used extensively to calculate complex single-phase[2,15] and two-phase[3] three-dimensional flowfields in an aircraft engine combustor. The code has the capability of analyzing the complex geometrical details of a modern gas turbine combustor, including the swirl cup, splash plate, primary and secondary dilution holes, film cooling slots, and multihole cooling zones. CONCERT calculates the mean velocity and turbulence field (using a standard $k$-$\varepsilon$ turbulence model) that are required by the composition PDF module. The choice of composition-only PDF was made over the joint velocity–composition PDF because the former could very easily be integrated with the CONCERT code. Also, since the computer time requirements for the three-dimensional calculations were going to be quite substantial anyway, it was felt that, initially, the composition-only PDF should be considered. The PDF transport equation was solved using a Lagrangian particle-tracking MC method. By performing ensemble averages of the particles in each computational cell, the mean density field is obtained and supplied to the CONCERT code.

The overall calculation procedure was validated against experimental data in a recirculating bluff-body stabilized CO/$H_2$/$N_2$ flame in which Raman measurements were made by Correa and Gulati.[16] Even though the geometry is two-dimensional axisymmetric, calculations were performed using the three-dimensional code by placing a minimum number of cells in the third direction. The computed mixture fraction and its variance (assuming fast chemistry) showed very good agreement with the data. As an initial demonstration of this hybrid MC/CONCERT CFD code as a production tool, a three-dimensional single cup section of a modern aircraft engine combustor was analyzed. Numerical solutions for this combustor were obtained on a Cray C-90 supercomputer and a Hewlett–Packard (HP) workstation, and the results obtained were compared with those calculated using the original assumed-shape PDF approach. Comparisons were also made with historical thermocouple data.

## Methodology

The hybrid MC/CONCERT CFD code consists of three separate modules that interface and communicate with each other via Fortran common blocks. The three modules are, respectively, 1) the chemistry and mixing module, 2) the particle tracking module, and 3) the gas velocity (i.e., CFD) module. Figure 1 outlines the flow of information between the modules. In the PDF transport method, the scalar PDF is discretized into

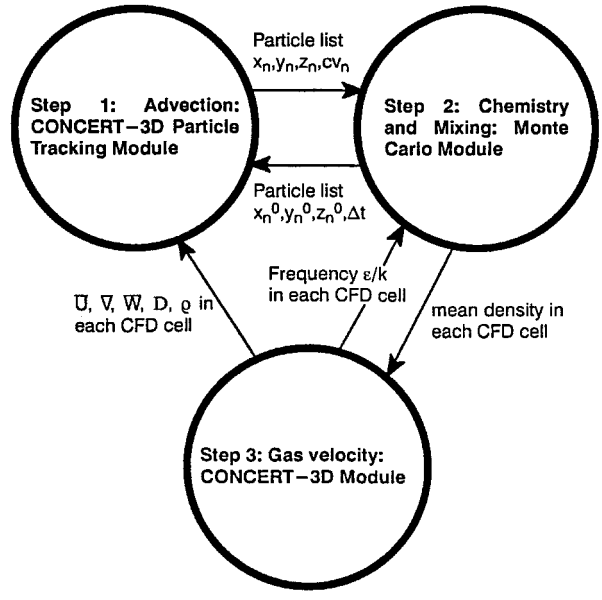


**Fig. 1 Schematic of communications within the modules of the hybrid CONCERT/MC code.**

equal particles. These particles carry with them a certain number of attributes that are convected and diffused through the entire computational domain based on the mean gas velocity field and the diffusion parameters. These particles also interact with each other and this interaction depends strictly on the turbulent mixing. The particle array $f(n, m)$ describes the composition completely. In this notation, $n$ is the particle index ($n = 1, 2, \ldots, N_p$, where $N_p$ is the total number of particles) and $m$ is the attribute number. The particle attributes tracked are density and the scalars that define the chemistry. From the list of particles present in a computational cell, the PDF of a particular attribute can be obtained in the cell. Thus, instead of assuming a shape for the PDF, it is actually computed by this method. In what follows, each of these modules together with their functions will be described.

### Chemistry/Mixing Module

The chemistry module (CM) is the one that changes the scalar attributes of each particle based on chemistry and mixing. An ordinary differential equation is solved for each particle and scalar attribute. Turbulent mixing is modeled by the interaction by exchange with the mean model.[17] The differential equation has the following form[18,19]:

$$\frac{\mathrm{d}Y_k^n}{\mathrm{d}t} = -\omega(Y_k^n - \bar{Y}_k) + w_k$$

where $Y_k^n$ is the magnitude of the scalar attribute $k$ corresponding to the particle $n$, $Y_k$ is the mean value of the attribute in the computational cell in which the particle resides, $\omega$ is given by $\varepsilon/k$, provided by the gas velocity module, and $w_k$ is the source term that represents the chemical reaction rate for that attribute. In this model, the particles do not interact with each other, but interact only with the mean (within the computational cell in which the particle is present). This mean magnitude of the attribute in a cell is obtained by performing an ensemble-weighted average over all of the particles in that cell. At the end of each time step, the particle field provides a snapshot of the chemistry/PDF distribution. An important strategy was used to improve the statistics. This ensemble average is computed as a running average over time steps (after stochastic convergence), which has the consequence of increasing the number of effective particles used in computing the PDF distribution. In a fast chemistry calculation, only the mixture fraction attribute of the particle is solved for and, consequently,

$w_k$ is zero. To perform finite rate chemistry calculations, reactive scalars (e.g., fuel mass fraction, and CO mass fraction, etc., depending on the chemistry scheme) must also be considered and will have nonzero source terms. For equilibrium chemistry, the density vs mixture fraction relationship is known for a given fuel, and so from a knowledge of the mixture fraction attribute of a particle, its density attribute is also obtained. After the mean density in each cell is computed, it is passed to the CFD module. The CM module works strictly with the list of particles, and does not actually require any information about the geometry (other than the index of the cell in which each particle resides, which is provided by the particle-tracking module).

**Particle Tracking Module**

The particle tracking (PT) module is set up to repetitively do the following prototypical initial value problem: given the starting particle positions $(x_n^0, y_n^0, z_n^0)$ and the size of $\Delta t$, it returns the new position $(x_n, y_n, z_n)$ and the corresponding control volume index at the end of the time step. The control volume index is simply an integer that identifies its location in space. Within the particle tracking module, time steps smaller than $\Delta t$ are taken to accurately obtain the particle trace. The magnitude of $\Delta t$ is chosen to be one-quarter of the residence time in a computational cell. The residence time is, of course, the ratio of the cell dimension to a representative velocity in the cell. By averaging the values of $\Delta t$ for each cell, a single value of $\Delta t$ is selected for the entire computation. Convection of the particles takes place with the velocity field given by $(\bar{V} + \underline{\text{grad}}\ \mu_T/\bar{\rho})$, where $\bar{V}$ is the mean velocity vector. This additional term $\underline{\text{grad}}\ \mu_T/\bar{\rho}$ is the drift correction that is required in an explicit particle tracking scheme.[20] Diffusion of the particles is controlled by the term that models the random walk (stochastic fluctuations) as the particles move through the domain. This walk is random in all three velocity directions and is assumed to be isotropic, possessing a Gaussian probability distribution in the fluctuating displacement. This displacement has a standard deviation, given by Brownian motion theory to be $(D\Delta t)^{1/2}$, where $D = 2\mu_T/\bar{\rho}$.[20] The displacements in the three directions are uncorrelated, i.e., three different random numbers are used to compute each instantaneous displacement component. The particles reflect perfectly off walls and symmetry boundaries, whereas, if they reach a periodic boundary, they reappear at the opposing periodic surface. At the inlets, the incoming mass flow is discretized into particles in such a way that the same number of particles enter from each inlet cell, but their weights are adjusted to reflect the mass flow. The scalar attributes of the particles are set according to whether the inlet stream is fuel or air or is premixed.

**CFD Module**

The gas phase velocity field is computed by the CONCERT-3D CFD code. The standard $k$-$\varepsilon$ turbulence model is used with wall function treatment for near-wall regions. The governing equations of motion (continuity, three momentum equations, and the two turbulence equations) are transformed from, in general, an arbitrarily-shaped physical domain to a rectangular parallelopiped. The equations are solved in this boundary-fitted coordinate system. After making finite difference approximations to the equations, they are solved on a staggered grid by a SIMPLE-like algorithm,[21] extended to the curvilinear coordinate system. The governing equations together with their discretization and the numerical algorithm have been described in detail.[22,23]

Figure 1, as mentioned earlier, gives a pictorial representation of the communication between the modules. In the serial implementation, the modules are run in the following sequence: the CFD module is run for 100–200 iterations (assuming constant density) that provides a provisional gas velocity field that is supplied to the particle tracking module. The mixing frequency $\varepsilon/k$, which is also obtained at the same time, is passed to the chemistry module. An initial ensemble of particles is specified cell-by-cell, with an equal number of particles in each cell and the weight of the particles within a cell proportional to the product of the density and volume of the cell. The initial scalar attribute of each of these particles is set equal to the initial value of the scalar (which, in fact, may be zero) in which the particle resides. The particle tracking and chemistry modules are advanced 20–50 time steps. At each time step, a fixed number of particles enter from the inlets while all of the particles within the domain are transported around in both physical and composition space (some particles leave the domain through the exits). At the end of the 20–50 time steps, a new density field is computed. At this point, one cycle of the calculations is complete. At the beginning of the next cycle, this new density field is used by the CFD module to recompute the gas velocity field and the entire process repeats thereon. A stochastic steady-state solution (fixed number of particles in the domain, and constant ensemble averages of the attributes within the domain as well as at the exit) was typically achieved in about 10–25 cycles of the computations. The usual CFD convergence criteria were employed for the momentum and continuity equations in determining complete convergence of the solution.

## Results

As stated earlier, the code was initially validated against benchmark-reacting flow data. The configuration chosen was a bluff-body stabilized nonpremixed axisymmetric $CO/H_2/N_2$–air flame within which Raman data has been taken by Correa and Gulati.[16] Figure 2 shows a schematic sketch of the burner. Assumed-shape PDF calculations were performed[16] and a two-dimensional joint velocity-composition PDF calculation with finite rate chemistry was performed[7] and compared with the data. Before embarking on this exercise, it was decided to develop a single three-dimensional code to perform this calculation as well as the aircraft engine combustor calculation. Even though the geometry is two-dimensional axisymmetric, the bluff body was modeled in this study as a three-dimensional object by generating a polar grid with a 15-deg sector angle. In this paper, fast chemistry calculations will be reported. The computed mean mixture fraction and its rms were compared with the data. The fuel jet velocity was 80 m/s; the rest of the flow conditions are shown in Fig. 2. The grid used for this calculation was the same as the one that was employed in Refs. 7 and 16. It is a nonuniform rectilinear mesh with 75 cells in the axial direction, and 60 cells in the radial direction. In the axial direction, the mesh grows with an expansion ratio of 2%, whereas in the radial direction this ratio is 3%. The mesh extends to 55 jet diameters along the axis and up to the tunnel wall along the radius. The solution of this two-dimensional problem using the three-dimensional CONCERT code required that at least three cells be placed in the angular direction. Calculations for this problem were carried out on an HP-735 workstation under the following conditions: 1170 incoming particles per time step, 243,000 initial particles in the domain, $\Delta t = 0.1$ ms, a total of about 335,000 particles in the domain at stochastic steady state, and $nstep = 15$. This works out to be an average of 25 particles per cell, which is the same as the number of particles per cell used in Ref. 7. The parameter *nstep* requires explanation. In the PT module, when a particle is advanced in space within a cell, the incremental distance it traverses at each step is $L_{\text{diag}}/nstep$, where $L_{\text{diag}}$ is the mean length of the cell diagonal. Therefore, in essence, *nstep* is an internal tracking parameter, which ensures that time steps smaller than $\Delta t$ are taken to obtain an accurate representation of the particle trace within the given time step. The total number of particles in the domain is kept under control by a number control routine in the CM module. If too many particles build up in a cell, they are clustered, whereas if there are too few particles in a cell, they are split to create more particles. In either situation, the particle weights are appropriately ad-

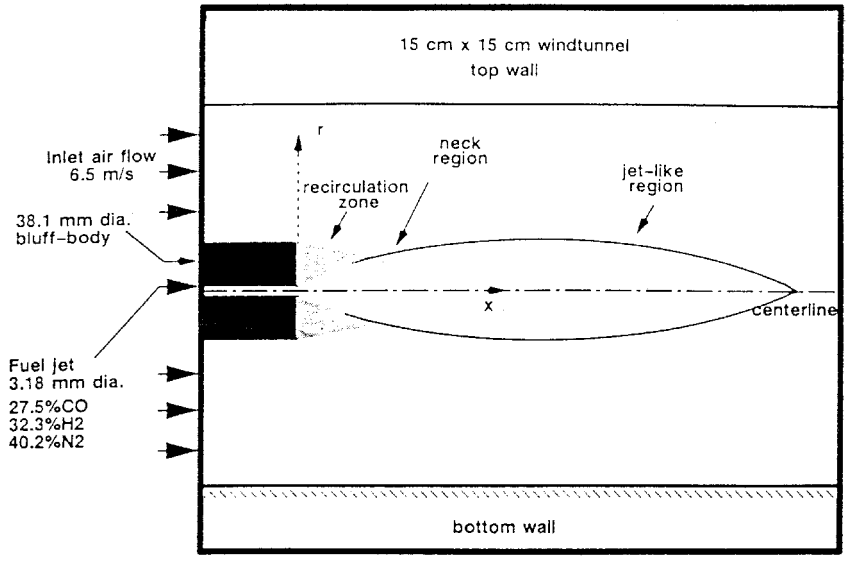


**Fig. 2 Schematic of the bluff-body stabilized burner in the tunnel, and regions of the flame.[16]**

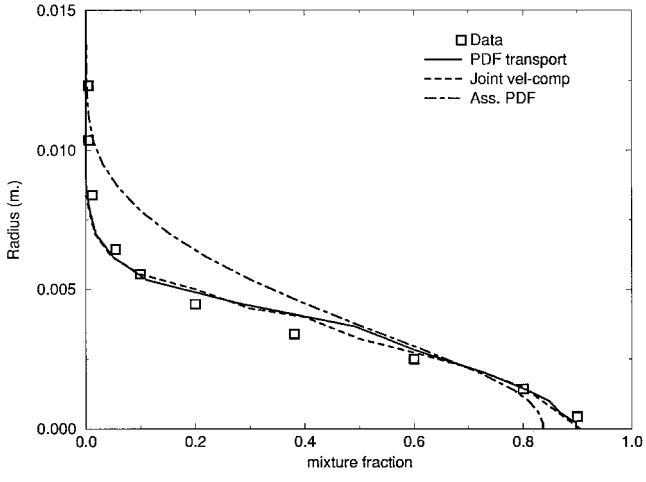


**Fig. 3 Predictions of the radial distribution of the mixture fraction at $x/d$ = 10, compared to data.**

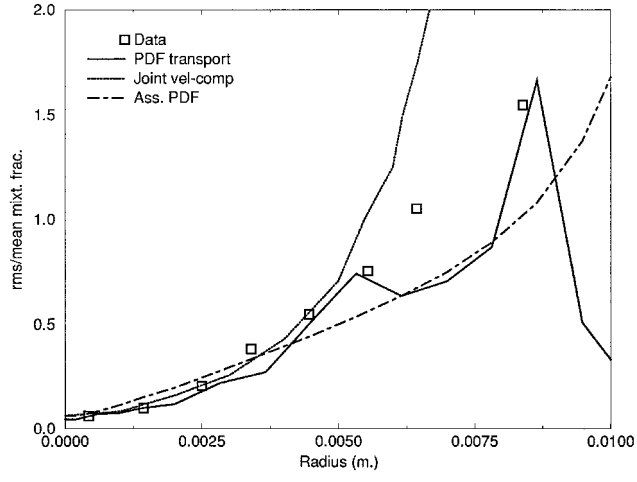


**Fig. 4 Predictions of the radial distribution of the rms of mixture fraction at $x/d$ = 10, compared to data.**

justed. While performing the clustering/splitting, the mean, variance, and other attributes within a cell are preserved so that the physics remains unchanged. There is a set maximum number of particles per cell that bounds the total number of particles in the domain. One complete cycle for this case comprised 200 CFD iterations and 30 time steps through which the PT/CM modules were advanced. A total of 20 cycles was required to achieve convergence with a total HP-735 CPU time of 16.3 h. Out of this 48.5% of the time was spent in the CFD module, 6.2% of the time was spent in the CM module, and the rest of the time (45.3%) was spent in the PT module. A calculation was also performed with 60% more particles, i.e., 540,000 particles in the domain. The results obtained were equivalent to the results shown in Figs. 3–6, proving that the number of particles used is sufficient.

Figure 3 shows the radial mixture fraction distribution at the axial location of $x/d$ = 10. This figure (in addition to all of the figures that follow) displays the result from the present PDF transport calculation together with the profile obtained from the two-dimensional joint velocity–composition PDF calculation made in Ref. 7. Also shown is the result from an assumed-shape PDF computation. The PDF transport solution shows excellent agreement with the data both near and away from the centerline with slight overprediction in between. The width is well predicted. The joint velocity–composition calculation also shows equivalent agreement at this location. The assumed-shape PDF model significantly overpredicts the mixture fraction away from the centerline, and is underpredicted near and at the centerline. Figure 4 compares the rms of mixture fraction at $x/d$ = 10, normalized by the mean. Once again, the present calculation together with the joint velocity–scalar calculation show very good agreement with the data, except in the outer edges where the mean itself is very small. The assumed-shape PDF calculation shows reasonable agreement near the jet centerline, but deviates below the data further away from the center. Figure 5 shows the mean mixture fraction profile at $x/d$ = 20. Here, it appears that the mixture fraction is somewhat overpredicted by the PDF transport model near the centerline and is underpredicted away from the center. The joint velocity–composition calculation also appears to show the same characteristics. The assumed-shape PDF computation overpredicts the mixture fraction for the most part, except near the centerline. Figure 6 compares the rms of mixture fraction at $x/d$ = 40, again normalized by the mean. At this location, both the PDF transport and the assumed-shape PDF approaches show good agreement with the data. In general, it may be concluded that the level of agreement with the present PDF transport technique is better than that obtained with the assumed-shape PDF model. This fact together with the observation that the present composition-only PDF method has the same level of agreement as the two-dimensional joint velocity–composition PDF model, suggests that the substantially added computational

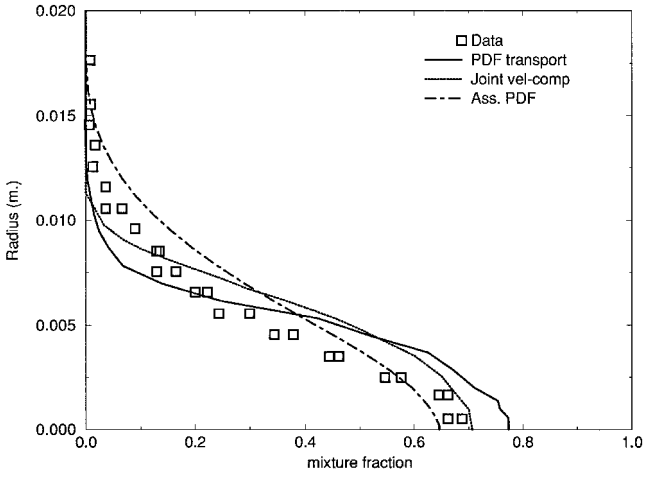


**Fig. 5 Predictions of the radial distribution of the mixture fraction at $x/d$ = 20, compared to data.**

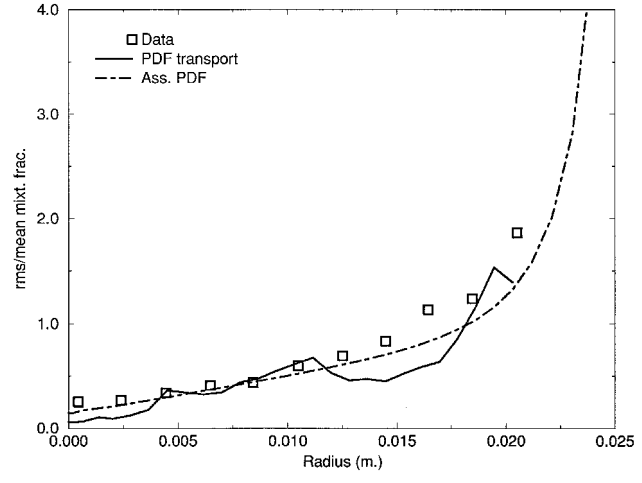


**Fig. 6 Predictions of the radial distribution of the rms of mixture fraction at $x/d$ = 40, compared to data.**

cost associated with a three-dimensional joint velocity–composition approach may be unnecessary and not justifiable at this time for production-type combustor calculations on large grids and several million MC particles.

Figure 7 shows a schematic of a modern aircraft engine combustor. It is of single annular design with 20 swirl cups equally spaced around the circumference. Each single-cup section contains 10 dilution holes (five top and five bottom) and 13 film cooling slots (seven top and six bottom) along the liner walls. The operating conditions are high power corresponding to sea-level takeoff (approximately 27 atm). The distributions of the mass flows[3] through the swirl cup, splash plate, film-cooling slots, and dilution holes are 18, 13, 39, and 30%, respectively. The mesh generated to model this combustor had a total of 58,621 grid points (54,000 computational cells). Based on past experience,[1–4] a mesh of this size has been found to be sufficient to resolve the combustor flowfields for most practical design purposes. On this grid, there are 376 cells through which flow enters the combustor from the swirl cup boundary, 260 inflow cells (film cooling holes and slots) on the inner boundary and 290 inflow cells on the outer boundary. Calculations using the PDF transport model with fast chemistry (Jet A fuel) were performed under the following conditions: 4630 incoming particles per time step, 702,000 initial particles in the domain, $\Delta t$ = 0.1 ms, and *nstep* = 3. One complete cycle consisted of 200 CFD iterations and 30 time steps through which the PT/CM modules were advanced. After particle clustering/splitting, the total

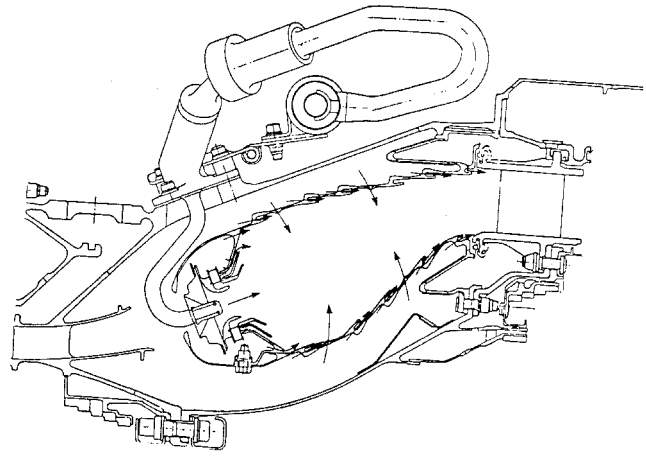

**Fig. 7 Geometry of a typical single annular aircraft engine combustor.**

number of particles in the domain reached a steady number of 1.08 million. As stated earlier, ensemble averaging of the particle attributes was performed over the last 30 time steps. Thus, the number of effective particles is over 32 million. A total of 20 cycles was required. This calculation was initially performed on a Cray C-90, and required a total CPU time of 42.8 h. Out of this, 2.4 h were spent in the CFD module, 28 min in the CM module, and 39.9 h in the PT module. The assumed-shape PDF calculation with CONCERT alone required 1.45 Cray C-90 h. The same calculation was performed on an HP-735 workstation, where it required 61.8 h of CPU time with the following distribution: 22.5 h in the CFD module, 2.32 h in the CM module, and 37.0 h in the PT module. (On the HP-735, the assumed-shape PDF calculation needed 14.7 h.) The reason for this lopsided distribution of the CPU time between the Cray and the HP-735 will be given in the next paragraph.

The CONCERT-3D CFD module that solves a series of transport equations has been vectorized well[3] for optimized processing on a supercomputer. However, several unavoidable dependencies concerning each particle (e.g., the special adjustments that have to be made when a particle hits a wall or other boundaries or when a particle crosses from one cell to the next, etc.) inhibit vectorization of the overall particle tracking loop. It is for this reason that the CFD module runs much faster on a machine with a vector processor, but the PT module performs poorly. This is the explanation for the majority of the time being spent in the PT module on the Cray. However, the HP-735 does not have a vector processor, and as such, the CFD module requires more CPU time and compared to that needed by the PT module. However, the particle tracking process in physical space is parallelizable since the particles do not interact with each other and they each traverse the domain independently. With this in mind, the particle-tracking code was rewritten to take advantage of the multitasking option on the Cray C-90. This required calls to be made to a number of Cray library routines and placement of loops over several portions of the code with these loops running over particles. The Cray C-90 that was employed has a total of six CPUs (processors). In multitasking the PT module, the particle tracking task is distributed between the CPUs. In an ideal situation when no other jobs are running on the machine and all CPUs are available, each CPU will be working in parallel and with its own particle list resulting in peak performance. However, in practice, there are several other jobs competing for the same resources and the performance achieved is less than the maximum. Nevertheless, multitasking has the potential of reducing the wall clock time on the Cray, but it would depend on the rest of the machine load. This very idea can also be incorporated on a cluster of workstations networked in parallel. On

such a network, it is possible to divide the particle list equally between the workstations, enabling quicker turnaround. The advantage of a workstation cluster over the Cray CPUs is that each workstation can dedicate itself entirely to its own particle tracking task with no other processes in competition. It might well be that a dedicated workstation network is the best platform for performing MC simulations. We are currently studying this approach.

Figure 8 shows the velocity vectors in a side-view plane in line with the swirl cups. The primary dilution hole flows from the inner and outer walls interact with each other as well as with the flow from the swirl cups, resulting in the establishment of a recirculation zone for the flame. The solution obtained using the PDF transport method is very similar in character to that obtained using the assumed-shape PDF method. From past experience with the assumed-shape PDF method, it has been observed that the best agreement with exit temperature data is obtained with a value of 0.5 for $Sc$.[24] Figure 9 is the temperature field in the same side-view plane as obtained by the assumed-shape PDF method ($Sc$ = 0.5), and again, by the PDF transport method. It should be noted that the effective $Sc$ in the PDF transport calculation described so far is 1.0. Figure 10 shows the temperatures in the exit plane as obtained by the two methods. From Fig. 9, it can be observed that the highest temperature within the combustor is predicted to be about 150 K greater by the PDF transport model, its location is slightly displaced but is in the same general region between the secondary dilution jets. The highest temperature at the exit occurs near the center between the outer and inner walls. The PDF transport solution is slightly less diffusive and predicts this peak combustor exit temperature to be higher by about 50 K.

To further understand the differences in the exit temperature predictions, it was decided to incorporate the $Sc$ in the PDF transport model and study its effect on the solution. This was done in the following manner. Diffusion of the particles is controlled by the random walk that is given by the term $(D\Delta t)^{1/2}$. In the assumed-shape PDF model, gradient transport of the mixture fraction is modeled using the diffusion coefficient $\mu_T/Sc$. Therefore, to produce the same effect, the random walk was replaced by $(D\Delta t/Sc)^{1/2}$. Figures 9 and 10 also show the solutions obtained by the PDF transport model at a $Sc$ of 0.5. As seen from Fig. 9, the highest temperature calculated within the combustor with $Sc$ = 0.5 is about the same as that computed using $Sc$ = 1.0, but this peak temperature region is smaller in size. The maximum temperature at the exit with $Sc$ = 0.5 (PDF transport) is observed to be about 100 K higher than that computed with $Sc$ = 1.0; however, the average temperature decreases, which will be seen in Fig. 11.

Figure 11 compares the circumferentially-averaged temperatures (in terms of the pattern factor: nondimensional temperature) with data taken by a thermocouple rake. Circumferential averaging removes any cup-to-cup variation in the numerical solutions. The assumed-shape PDF solution overpredicts the temperature in the outer half, while underpredicting it in the inner half of the exit. The temperature from the PDF transport solution ($Sc$ = 1) appears to agree with the data close to the outside wall, but overpredicts it significantly along the rest of the annulus. However, at the $Sc$ of 0.5, the temperature from

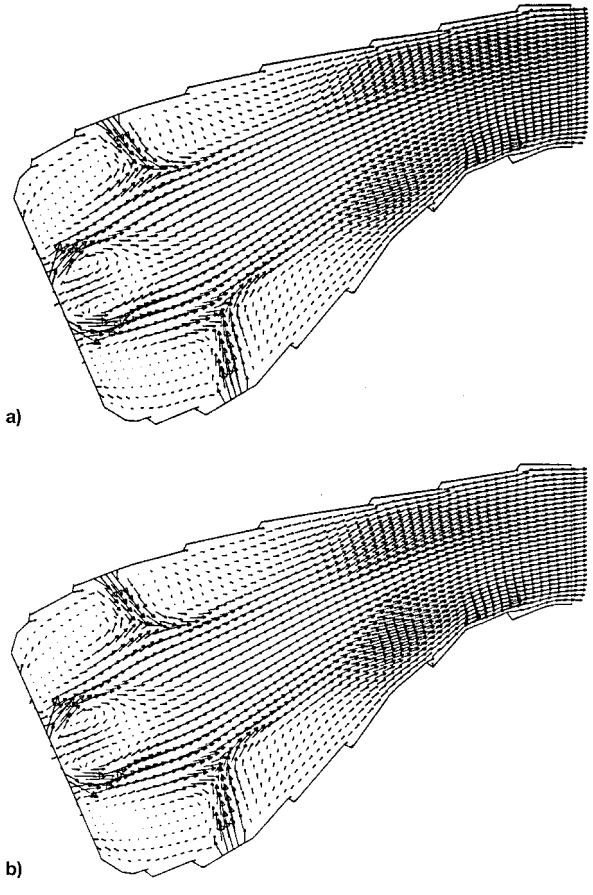


**Fig. 8 Projected velocity vectors in a side view through the swirl cup of the engine combustor a) assumed-shape PDF approach and b) PDF transport approach.**

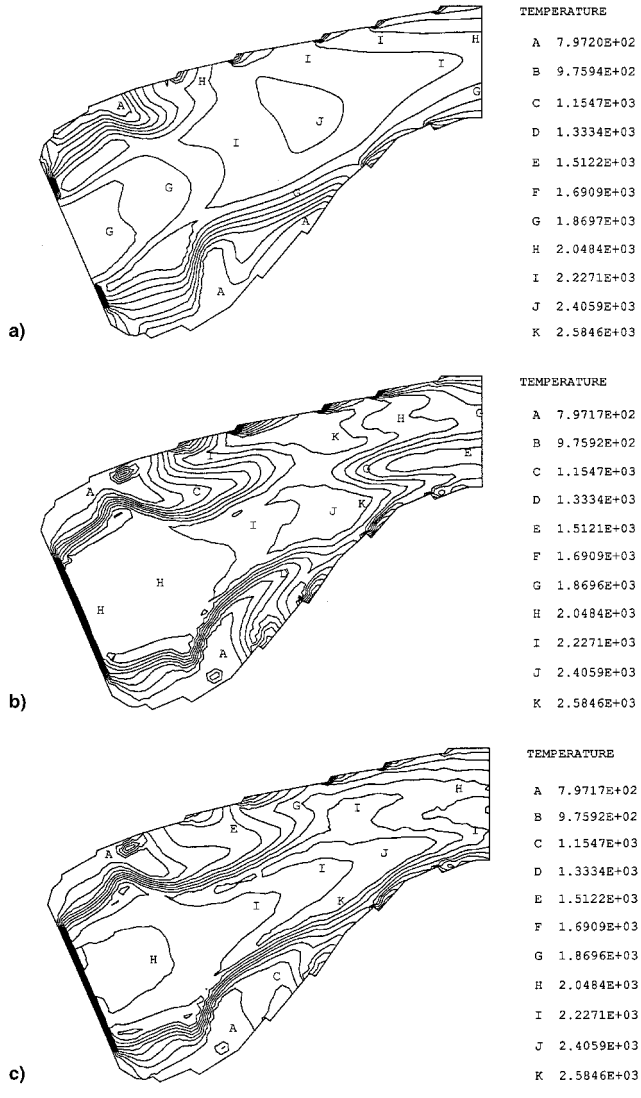


**Fig. 9 Calculated temperature contours (K) in a side view through the swirl cup of the engine combustor a) assumed-shape PDF with $Sc$ = 0.5; and b) PDF transport at values of $Sc$ = 1.0 and c) 0.5.**

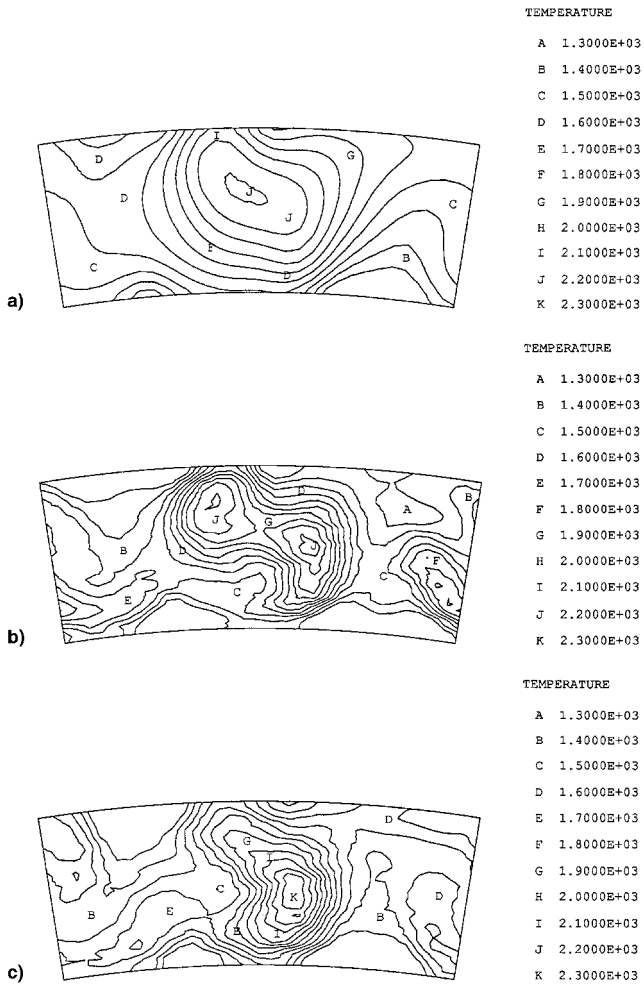


**Fig. 10 Calculated temperature contours (K) at the exit of the engine combustor a) assumed-shape PDF with *Sc* = 0.5; and b) PDF transport at values of *Sc* = 1.0 and c) 0.5.**

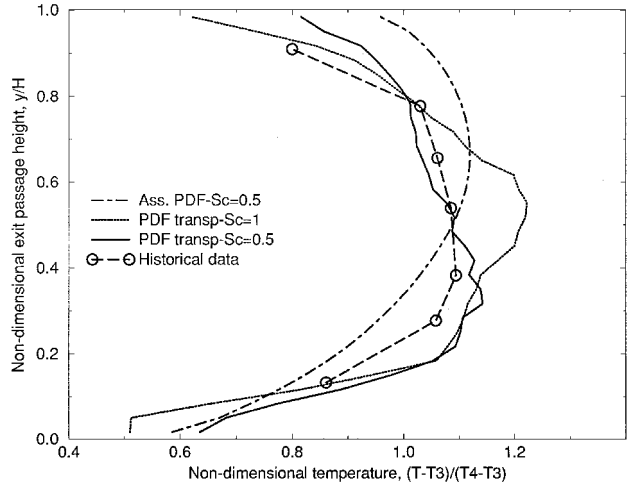


**Fig. 11 Calculated exit radial temperature profiles (circumferentially averaged and in terms of the pattern factor) from the assumed-shape PDF and PDF transport approaches compared with each other and thermocouple data.**

the PDF transport solution shows very good agreement with the data along most of the annulus, except near the inner wall where it is slightly higher. On an overall basis, relative to the assumed-shape PDF method, the PDF transport solution indicates better agreement with the data. When this model is applied for production combustor calculations, some amount of calibration of the input parameters such as the *Sc* may have to be performed.

## Conclusions and Future Directions

A Lagrangian PDF transport model has been coupled with a three-dimensional body-fitted CFD code (CONCERT-3D). The development of the PDF model is highly modular, enabling its interface with any CFD code. Predictions of the mixture fraction and its variance made by the model indicated excellent agreement with corresponding bluff-body reacting flow Raman data. Three-dimensional flow calculations have been successfully performed with fast chemistry in a real piece of combustion hardware, a single annular aircraft engine combustor. The PDF transport approach takes more computer time than conventional CFD methods. On the Cray, the particle-tracking algorithm has been written to run in parallel on the different processors (multitasking). Efforts to run the particle-tracking module on a parallel network of workstations are underway. The temperature field calculated by the PDF transport code showed the peak temperature level within the combustor and its location to be about the same as the assumed-shape PDF approach. At the exit plane, the PDF transport approach (*Sc* = 1) predicts a somewhat higher temperature relative to the assumed-shape PDF method. When the *Sc* was lowered to 0.5, the predicted temperature decreased. The comparison with the exit temperature data also showed far better agreement with *Sc* = 0.5.

The advantage of the PDF transport method is the ability to make accurate predictions of CO, UHC, $NO_x$, and other emissions, since their PDFs are actually computed by this model. To effect this, multiple scalars (conserved scalar + additional reactive scalars) and reduced chemistry schemes have to be incorporated. Implementation of schemes for hydrocarbons is presently underway and will be reported in a future paper. The reactive scalars have nonzero source terms whose values have to be either analytically defined or obtained by first reading in thermochemical tables and devising efficient table lookups.

## Acknowledgment

The authors wish to acknowledge the contribution of Glenn Wehrer of Cray Research who was largely responsible for implementing multitasking in the particle-tracking module for the Cray C-90.

## References

[1]Correa, S. M., and Shyy, W., "Computational Models and Methods for Continuous Gaseous Turbulent Combustion," *Progress in Energy Combustion Science*, Vol. 13, 1987, pp. 249–292.

[2]Shyy, W., Correa, S. M., and Braaten, M. E., "Computation of Flow in a Gas Turbine Combustor," *Combustion Science and Technology*, Vol. 58, 1988, pp. 97–117.

[3]Tolpadi, A. K., "Calculation of Two-Phase Flow in Gas Turbine Combustors," *Journal of Engineering for Gas Turbines and Power*, Vol. 117, 1995, pp. 695–703.

[4]Gulati, A., Tolpadi, A. K., VanDeusen, G., and Burrus, D., "Effect of Dilution Air on Scalar Flowfield at Combustor Sector Exit," *Journal of Propulsion and Power*, Vol. 11, No. 6, 1995, pp. 1162–1169.

[5]Pope, S. B., "Computations of Turbulent Combustion: Progress and Challenges," *23rd International Symposium on Combustion*, The Combustion Inst., Pittsburgh, PA, 1990, pp. 591–612.

[6]Anand, M. S., Pope, S. B., and Mongia, H. C., "Pressure Algorithm for Elliptic Flow Calculations with the PDF Method," CFD Symposium on Aeropropulsion, NASA Lewis Research Center, 1990.

[7]Correa, S. M., and Pope, S. B., "Comparison of Monte Carlo PDF/Finite Volume Mean Flow Model with Bluff Body Raman Data," *24th International Symposium on Combustion*, The Combustion Inst., Pittsburgh, PA, 1992, pp. 279–285.

[8]Pope, S. B., and Correa, S. M., "Joint PDF Calculations of a Non-Equilibrium Turbulent Diffusion Flame," *21st International Symposium on Combustion*, The Combustion Inst., Pittsburgh, PA, 1986, pp. 1341–1348.

[9]Anand, M. S., and Pope, S. B., "Calculations of Premixed Com-

bustion Flames by PDF Methods," *Combustion and Flame*, Vol. 67, 1987, pp. 127–142.

[10]Chen, J. Y., and Kollmann, W., "PDF Modeling of Chemical Nonequilibrium Methods in Turbulent Nonpremixed Hydrocarbon Flames," *22nd International Symposium on Combustion*, 1988, pp. 645–653.

[11]Chen, J. Y., Kollmann, W., and Dibble, R. W., "PDF Modeling of Turbulent Nonpremixed Methane Jet Flames," *Combustion Science and Technology*, Vol. 64, 1989, pp. 315–346.

[12]Chen, J. Y., Dibble, R. W., and Bilger, R. W., "PDF Modeling of Turbulent Nonpremixed $CO/H_2/N_2$ Jet Flames with Reduced Mechanisms," *23rd International Symposium on Combustion*, 1990, pp. 775–780.

[13]Chen, J. Y., and Kollmann, W., "PDF Modeling and Analysis of Thermal NO Formation in Turbulent Nonpremixed Hydrogen–Air Jet Flames," *Combustion and Flame*, Vol. 88, 1992, pp. 379–412.

[14]Leonard, A. D., and Dai, F., "Applications of a Coupled Monte Carlo PDF/Finite Volume CFD Method for Turbulent Combustion," AIAA Paper 94-2904, June 1994.

[15]Shyy, W., Tong, S. S., and Correa, S. M., "Numerical Recirculating Flow Calculations Using a Body-Fitted Coordinate System," *Numerical Heat Transfer*, Vol. 8, 1985, pp. 99–113.

[16]Correa, S. M., and Gulati, A., "Measurements and Modeling of a Bluff Body Stabilized Flame," *Combustion and Flame*, Vol. 89, 1992, pp. 195–213.

[17]Borghi, R., "Turbulent Combustion Modeling," *Progress in Energy and Combustion Science*, Vol. 14, 1988, pp. 245–292.

[18]Correa, S. M., "Turbulent-Chemistry Interactions in the Intermediate Regime of Premixed Combustion," *Combustion and Flame*, Vol. 93, 1993, pp. 41–60.

[19]Correa, S. M., and Braaten, M. E., "Parallel Simulations of Partially Stirred Methane Combustion," *Combustion and Flame*, Vol. 94, 1993, pp. 469–486.

[20]Pope, S. B., "PDF Methods for Turbulent Reactive Flows," *Progress in Energy and Combustion Science*, Vol. 11, 1985, pp. 119–192.

[21]Patankar, S. V., *Numerical Heat Transfer and Fluid Flow*, McGraw–Hill, New York, 1980.

[22]Tolpadi, A. K., and Braaten, M. E., "Study of Branched Turboprop Inlet Ducts Using a Multiple Block Grid Calculation Procedure," *Journal of Fluids Engineering*, Vol. 114, 1992, pp. 379–385.

[23]Shyy, W., and Braaten, M. E., "Three-Dimensional Analysis of the Flow in a Curved Hydraulic Turbine Draft Tube," *International Journal for Numerical Methods in Fluids*, Vol. 6, 1986, pp. 861–882.

[24]Burrus, D. L., "Application of Numerical Models for Predictions of Turbine Engine Combustor Performance," American Society of Mechanical Engineers, Paper 89-GT-251, June 1989.